Optimization-based Islanding of Power Networks using Piecewise Linear AC Power Flow

P. A. Trodden, *Member, IEEE,* W. A. Bukhsh, A. Grothey, and K. I. M. McKinnon

***Abstract*—In this paper, a flexible optimization-based approach to intentional islanding is presented. The decision is made of which transmission lines to switch in order to split the network while minimizing disruption, the amount of load shed, or grouping coherent generators. The approach, uniquely, considers voltages and reactive power directly when designing islands, since the optimization constraints include a piecewise linear model of AC power flow. Solution of the MILP provides islands that are balanced in real and reactive power, satisfy AC power flow laws, and have a healthy voltage profile.**

I. Introduction

The last decade has seen a number of notable cases of wide-area blackouts as a consequence of severe disturbances and cascading failures [1]–[3]. Although preventive and corrective systems exist to ameliorate the effects of severe disturbances, the operation of networks closer to limits, together with increased uncertainty in load and distributed generation, means that cascading failures may be harder to prevent, or stop once instigated [4]. Thus, intentional islanding is attracting attention as a corrective measure for limiting the effects of severe disturbances and preventing wide-area blackout.

Intentional islanding aims to split a network, by disconnecting lines, into electrically-isolated islands. The challenge is that, if an island is to be feasible, it must satisfy both static constraints—load/generation balance, network constraints, system limits—and dynamic constraints, *i.e.*, for frequency and voltage stability. Moreover, the act of islanding must not cause a loss of synchronism or voltage collapse. Many approaches have been proposed, *e.g.*, [5]–[11], each considering one or more, but not all, of these criteria when designing islands.

In [12], an optimization-based approach to islanding and load shedding was proposed. A key feature is that, unlike many other methods, it takes into account the part of the network that is desired to be isolated—*e.g.*, an impacted area—and determines how to isolate this while minimizing the amount of load shed or lost. The problem is formulated as a single mixed integer linear programming (MILP) problem, meaning that power balances, flows, and operating limits may be specified explicitly, and satisfied in each island in a feasible solution.

The islanding MILP problem has similarities with the *transmission switching* problem [13], in that the decision variable includes which lines to disconnect, while power flow constraints must be satisfied following any disconnection. Both approaches—islanding and transmission switching—may be seen as network topology optimization problems with added power flow constraints. In both cases, inclusion of AC power flow laws in the constraints results in a mixed integer nonlinear program (MINLP), which is difficult to solve. Hence, linear DC power flow has been used to date, resulting in a more computationally favourable MILP or MIQP problem.

A disadvantage of the DC power flow model is that the effect of line disconnections on network voltages is not considered. This is not exclusive to MILP-based islanding and transmission switching; a number of islanding approaches consider real power only, and assume that reactive power may be compensated locally after splitting. In [12], however, cases were reported where a solution could not be found to satisfy AC power flow and voltage constraints when the islands were designed considering DC power flow, *even when sufficient reactive power generation capacity was present in each island*. Investigation found that local shortages or surpluses of reactive power led to abnormal voltages in certain areas of the network.

This paper presents a flexible approach to the problem of designing system islands while considering voltage and reactive power. Firstly, a piecewise linear approximation to AC power flow is developed for use in power system optimization problems. This model is used in a MILP-based approach to islanding, where the decisions to make are which lines to disconnect, loads to shed and how to adjust generators in order to isolate a part of the network. Results obtained for test networks demonstrate the advantage of considering voltage and reactive power when deciding how to island, since instances of AC-infeasible islands are eliminated. The second contribution, when compared with [12], is flexibility in the definition of the area of the network to be isolated and the subsequent objective choice. For example, the objective may be to isolate an impacted area while minimizing the expected load shed or lost; or, it may be to split the network such that coherent synchronous machines remain in the same section.

The organization of this paper is as follows. The piecewise linear AC power flow model is presented, and its use is demonstrated in an Optimal Power Flow (OPF) problem. In Section III, the islanding formulation is described. Section IV presents computational results for test networks. Conclusions are made in Section V.

II. Piecewise Linear AC Power Flow

A. Notation

A network comprises a set of buses $\mathcal{B}$ and a set of branches $\mathcal{L}$. The vectors F and T describe the connection topology: branch $l \in \mathcal{L}$ connects bus F_l to bus T_l. The set of generators is $\mathcal{G}$ and the set of loads is $\mathcal{D}$. A subset $\mathcal{G}_b$ of generators is attached to bus $b \in \mathcal{B}$; similarly, a subset $\mathcal{D}_b$ of loads is present at bus $b \in \mathcal{B}$. Bus $b \in \mathcal{B}$ has a voltage magnitude v_b and phase angle δ_b. Branch l has conductance g_l, susceptance b_l, shunt susceptance b_l^{C}, and carries real (reactive) power flows p_l^{12} (q_l^{12}) from end 1 (bus F_l) to end 2 (bus T_l), and p_l^{21} (q_l^{21}) from end 2 to end 1. If branch l is a transformer, it has an off-nominal tap ratio of τ_l. The phase angle difference across l is

This work was supported by the UK Engineering and Physical Sciences Research Council (EPSRC) under grant EP/G060169/1.

P. A. Trodden is with the Department of Automatic Control & Systems Engineering, University of Sheffield, Mappin Street, Sheffield S1 3JD, UK (e-mail: p.trodden@shef.ac.uk).

W. A. Bukhsh, A. Grothey, and K. I. M. McKinnon are with the School of Mathematics, University of Edinburgh, James Clerk Maxwell Building, Edinburgh EH9 3JZ, UK (e-mail: w.a.bukhsh@sms.ed.ac.uk, a.grothey@ed.ac.uk, k.mckinnon@ed.ac.uk).

$\theta_l = \delta_{F_l} - \delta_{T_l}$. A generator $g \in \mathcal{G}$ has real and reactive power outputs p_g^{G} and q_g^{G} respectively. A load $d \in \mathcal{D}$ is supplied with real (reactive) power p_d^{D} (q_d^{D}).

B. Linearized AC power flow

The linear "DC" model is a widely accepted approximation to AC power flow, whose benefits (linearity, simplicity) outweigh its shortcomings. Recently, however, there has been renewed research interest in the DC model itself [14] and more accurate alternative linearizations [15]. Recent work [12] by the authors found that a DC-based approach to controlled islanding sometimes led to infeasible islands being created, mainly owing to out-of-bound voltages and local shortages or surpluses of reactive power. Motivated by this, this section presents a piecewise linear approximation to AC power flow, in which voltage and reactive power are modelled. The formulation models as piecewise linear, thus to arbitrary levels of accuracy, the cosine term that would be the dominant source of error in a standard linear formulation.

The AC power flow equations are described as follows. Real and reactive power balances at each bus $b \in \mathcal{B}$ give

$$\sum_{g\in\mathcal{G}_b} p_g^{\mathrm{G}} = \sum_{d\in\mathcal{D}_b} p_d^{\mathrm{D}} + \sum_{l\in\mathcal{L}:F_l=b} p_l^{12} + \sum_{l\in\mathcal{L}:T_l=b} p_l^{21} + G_b^{\mathrm{B}} v_b^2,$$
$$\sum_{g\in\mathcal{G}_b} q_g^{\mathrm{G}} = \sum_{d\in\mathcal{D}_b} q_d^{\mathrm{D}} + \sum_{l\in\mathcal{L}:F_l=b} q_l^{12} + \sum_{l\in\mathcal{L}:T_l=b} q_l^{21} - B_b^{\mathrm{B}} v_b^2,$$

where G_b^{B} and B_b^{B} are the shunt conductance and susceptance at bus b. The power flows through a branch $l \in \mathcal{L}$ are

$$p_l^{ij} = v_{F_l}^2 G_l^{ii} + v_{F_l} v_{T_l} \left(G_l^{ij} \cos\theta_l + B_l^{ij} \sin\theta_l\right),$$
$$q_l^{ij} = -v_{F_l}^2 B_l^{ii} - v_{F_l} v_{T_l} \left(B_l^{ij} \cos\theta_l - G_l^{ij} \sin\theta_l\right),$$

for $i, j \in \{1, 2\} : i \neq j$, and where G_l^{ij}, B_l^{ij} are elements of the admittance matrix $\mathbf{Y}_l = \mathbf{G}_l + \jmath\mathbf{B}_l$ between F_l and T_l:

$$\mathbf{G}_l = \begin{bmatrix} g_l \frac{1}{\tau_l^2} & -g_l \frac{1}{\tau_l} \\ -g_l \frac{1}{\tau_l} & g_l \end{bmatrix}, \quad \mathbf{B}_l = \begin{bmatrix} \left(b_l + \frac{b_l^{\mathrm{C}}}{2}\right)\frac{1}{\tau_l^2} & -b_l \frac{1}{\tau_l} \\ -b_l \frac{1}{\tau_l} & b_l + \frac{b_l^{\mathrm{C}}}{2} \end{bmatrix}.$$

The standard "DC" approximation to AC power flow linearizes these equations by using the approximations $v_{F_l} = v_{T_l} \approx 1$, $\sin\theta_l \approx \theta_l$, $\cos\theta_l \approx 1$, and $b_l \gg g_l \approx 0$ yielding $p_l^{ij} = B_l^{ij}\theta_l$ and $q_l^{ij} = 0$. In the linearization in this paper, voltage and reactive power are retained. First, define $y_l = \cos\theta_l$ and $z_l = \sin\theta_l$, so that

$$p_l^{ij} = v_{F_l}^2 G_l^{ii} + G_l^{ij} v_{F_l} v_{T_l} y_l + B_l^{ij} v_{F_l} v_{T_l} z_l,$$
$$q_l^{ij} = -v_{F_l}^2 B_l^{ii} - B_l^{ij} v_{F_l} v_{T_l} y_l + G_l^{ij} v_{F_l} v_{T_l} z_l,$$

then linearize these flows about $v_{F_l} = 1$, $v_{T_l} = 1$ and $\theta_l = 0$ (hence $y_l = 1, z_l = 0$).

$$\tilde{p}_l^{ij} = G_l^{ii}(2v_{F_l} - 1) + G_l^{ij}\left(v_{F_l} + v_{T_l} + y_l - 2\right) + B_l^{ij} z_l,$$
$$\tilde{q}_l^{ij} = B_l^{ii}(1 - 2v_{F_l}) - B_l^{ij}\left(v_{F_l} + v_{T_l} + y_l - 2\right) + G_l^{ij} z_l.$$

In a standard linearization, the small-angle approximations would then be used: $y_l = \cos\theta_l \approx 1$ and $z_l = \sin\theta_l \approx \theta_l$. For small angles, the errors in these approximations are of the order θ_l^2 and θ_l^3 respectively. It follows that the cosine term is the more dominant source of nonlinearity.

TABLE I
APPROXIMATION ERRORS IN LINE FLOW TERMS

Term	Approximation	Max abs error on $\mathcal{X}$
$v_{F_l}^2$	$2v_{F_l} - 1$	0.010
$v_{F_l} v_{T_l} y_l$	$v_{F_l} + v_{T_l} + y_l - 2$	0.036
$v_{F_l} v_{T_l} z_l$	z_l	0.105
y_l	1	0.134
z_l	θ_l	0.024

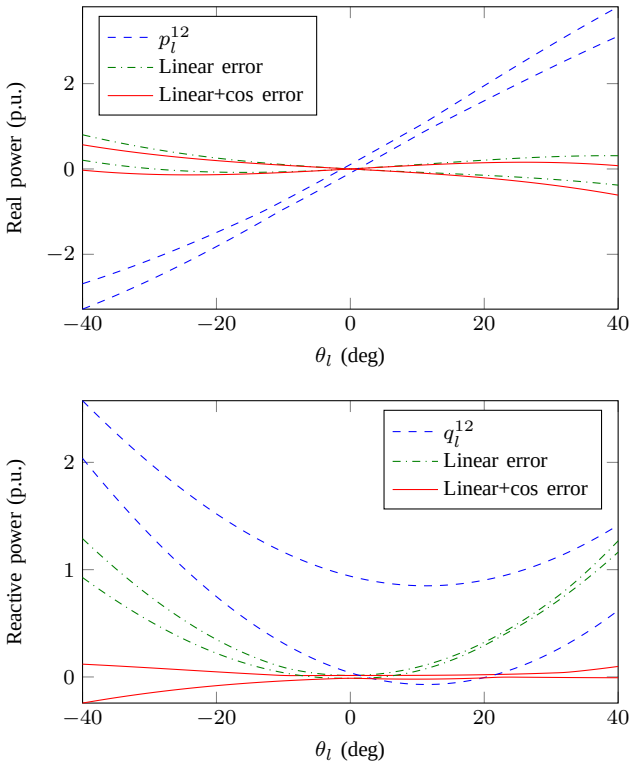

Fig. 1. Real and reactive power flows as a function of phase angle difference, for different bus voltages: AC flows (p_l^{12} and q_l^{12}; blue), and errors between AC flows and linearized flows (*i.e.*, $p_l^{12} - \tilde{p}_l^{12}$ and $q_l^{12} - \tilde{q}_l^{12}$) with $y_l = \cos\theta_l$ (green) and $y_l = 1$ (red).

To visualize the approximation errors, Table I gives the maximum absolute errors for each of the constituent terms in the linearized flows, over a typical range of operating voltages and angles. That is, the domain $\mathcal{X} = \left\{(v_{F_l}, v_{T_l}, \theta_l) : 0.9 \leq v_{F_l} \leq 1.1, 0.9 \leq v_{T_l} \leq 1.1, |\theta_l| \leq 30^\circ\right\}$. The cosine approximation incurs the largest error. Figure 1 then investigates errors over this domain for a line with properties $g_l = 1, b_l = -5, b_l^{\mathrm{C}} = 1$. The plots compare the approximation errors, $p_l^{12} - \tilde{p}_l^{12}$ and $q_l^{12} - \tilde{q}_l^{12}$, obtained when the $y_l = \cos\theta_l$ term is approximated as 1 (a linear model) and modelled exactly (linear plus cosine). In both cases, $z_l = \sin\theta_l \approx \theta_l$ is used. Although little reduction in errors is apparent in the real flows, the importance of modelling the cosine term is clear for reactive flows.

A similar analysis shows that including the sine term (instead of its linearization) in addition to the cosine term reduces the error in the real flows slightly, but makes no significant difference to the reactive power. Since the infeasibilities that occur using the DC approach to islanding are mainly owing

to the reactive power and voltage limits [12], the appropriate approximation to use is the linear plus cosine one. And although cosine terms cannot be used directly in an MILP model, they can be modelled to arbitrary levels of accuracy by piecewise linear functions. The next section demonstrates the use of the model in an OPF formulation.

C. Piecewise linear AC OPF

The piecewise linear (PWL) AC OPF problem is defined as

$$\min \sum_{g\in\mathcal{G}} c_g\big(p_g^{\mathrm{G}}\big) \tag{1}$$

subject to, $\forall b \in \mathcal{B}$, linearized Kirchhoff's current law:

$$\sum_{g\in \mathrm{G}_b} p_g^{\mathrm{G}} = \sum_{d\in\mathcal{D}_b} P_d^{\mathrm{D}} + \sum_{l\in\mathcal{L}:F_l=b} p_l^{12} + \sum_{l\in\mathcal{L}:T_l=b} p_l^{21} + G_b^{\mathrm{B}}(2v_b-1), \tag{2a}$$

$$\sum_{g\in \mathcal{G}_b} q_g^{\mathrm{G}} = \sum_{d\in\mathcal{D}_b} Q_d^{\mathrm{D}} + \sum_{l\in\mathcal{L}:F_l=b} q_l^{12} + \sum_{l\in\mathcal{L}:T_l=b} q_l^{21} - B_b^{\mathrm{B}}(2v_b-1). \tag{2b}$$

where P_d^{D} (Q_d^{D}) is the fixed real (reactive) power demand from load d. Line flow equations are included for all $l \in \mathcal{L}$ and $i, j \in \{1, 2\} : i \neq j$,

$$p_l^{ij} = G_l^{ii}(2v_{F_l}-1) + G_l^{ij}\big(v_{F_l}+v_{T_l}+y_l-2\big) + B_l^{ij}\theta_l \tag{3a}$$

$$q_l^{ij} = B_l^{ii}(1-2v_{F_l}) - B_l^{ij}\big(v_{F_l}+v_{T_l}+y_l-2\big) + G_l^{ij}\theta_l \tag{3b}$$

The N-piece PWL approximation to $(1-\cos\theta_l)$: $\forall l \in \mathcal{L}$,

$$y_l = c_{l,i}\theta_l + d_{l,i}, \forall \theta_l \in [x_{l,i}, x_{l,i+1}], i \in \{0,\dots,N-1\}, \tag{4}$$

where $c_{l,i}$ and $d_{l,i}$ are obtained by evaluating $\cos x$ at breakpoints $\{x_{l,0},\dots,x_{l,N}\}$.

System limits are applied:

$$V_b^{\min} \le v_b \le V_b^{\max}, \forall b \in \mathcal{B}, \tag{5a}$$

$$P_g^{\mathrm{G,min}} \le p_g^{\mathrm{G}} \le P_g^{\mathrm{G,max}}, \forall g \in \mathcal{G}, \tag{5b}$$

$$Q_g^{\mathrm{G,min}} \le q_g^{\mathrm{G}} \le Q_g^{\mathrm{G,max}}, \forall g \in \mathcal{G}. \tag{5c}$$

Line flow limits are applied by converting apparent power limits to heating limits. Supposing an MVA limit $S_l^{\max}$ is given, the constraint is formed by assuming nominal voltage and imposing an upper bound on the real loss $p_l^{12}+p_l^{21}$:

$$p_l^{12}+p_l^{21} \le \frac{g_l}{\big(g_l^2+b_l^2\big)}\Big(S_l^{\max}\Big)^2. \tag{5d}$$

1) Piecewise linear modelling of $\cos\theta_l$*:* The implementation of (4) requires binary variables to be introduced, either directly or indirectly. The overall problem is then , depending on the cost function c_g, a mixed integer linear or quadratic program (MILP or MIQP). The easiest, and preferred, way is to model with special ordered sets (SOS) of type 2 [16], which some solvers (*e.g.*, CPLEX) can handle directly and efficiently.

Because the OPF minimizes generation cost, then it also indirectly minimizes real power losses. The loss of a line l is proportional to $1-\cos\theta_l = 1-y_l$. Therefore, (4) could be replaced by

$$y_l \le c_{l,i}\theta_l + d_{l,i}, \forall i \in \{0,\dots,N-1\}, \tag{6}$$

which requires no SOS or binary variables, and maintains the OPF as an LP or QP. However, as the following example shows, the SOS formulation is essential in certain situations.

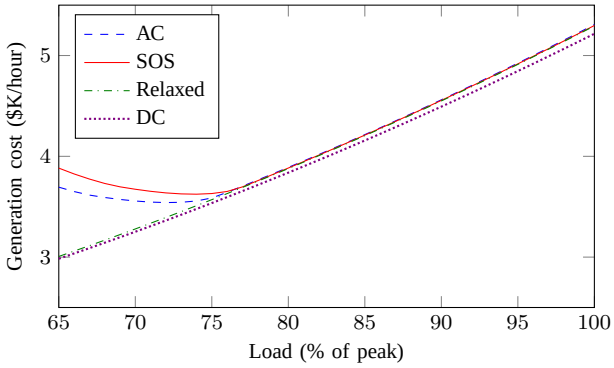

Fig. 2. Generation costs as a function of load for the 9-bus network.

An OPF was solved for the WSCC 9-bus system for a range of demands. A modification was made to the default network data [17]: voltage limits are set to $\pm 5\%$, and the lower limit on reactive power for each generator was changed from -300 to -5 MVAr. The PWL approximation used, for a line l, 20 pieces between $\pm\big(|\theta_l^*|+2^\circ\big)$, where θ_l^* is from the AC OPF solution. Fig. 2 shows the generation costs against load level, as obtained by AC, PWL with SOS (4), and relaxed PWL (6) OPFs. As the load percentage lowers, more of the lines are sources, rather than stores, of reactive power. The lower limits on reactive generation mean it becomes difficult for the generators to compensate, and the AC OPF shows that the generation cost increases. While the SOS PWL is able to capture this effect, the relaxed PWL "cheats" by having some lines continue to store reactive power despite their end voltages and phase angles—allowed because $y_l < c_{l,i}\theta_l + d_{l,i}$ is permitted.

2) Degeneracy of OPF: An AC OPF is in some situations nearly degenerate, since the cost is concerned only with where, and how much, real power is generated. Reactive power must balance, but its sources are less important. Real and reactive power flows are coupled, but entirely different reactive generator outputs and flows are often possible while leaving the real outputs, hence generation cost, and flows largely the same. The consequence is that while the optimal solutions to the AC and PWL problems might be close in cost and real flows, reactive flows and voltages may be significantly different, as shown by solving the respective OPF problems for the 24-bus Reliability Test System [18]. The 20-piece PWL OPF obtains a generation cost of \$63288, which when compared to the AC solution cost of \$63352, represents an underestimate of \$64, or 0.10%. By comparison, a DC OPF obtains \$61001, a 3.71% error. However, while the real flows and phase angles are similar, significant errors are apparent in the voltage profile (Fig. 3).

This is partly explained by the near-degeneracy of the AC

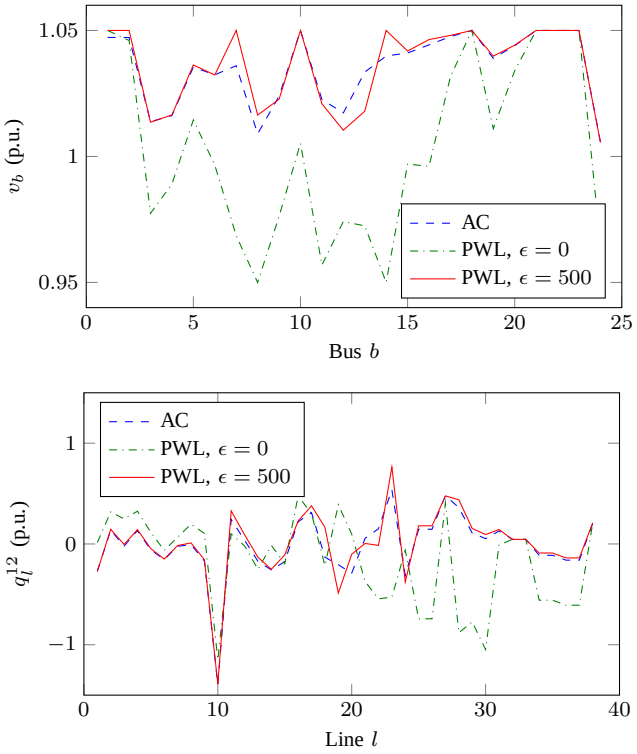

Fig. 3. Errors in voltage and reactive flows between AC and PWL OPF solutions ($v_b^{\text{AC}} - v_b^{\text{PWL}}$ and $(p_l^{12})^{\text{AC}} - (q_l^{12})^{\text{PWL}}$ respectively).

OPF problem, but also by the fact that the the linearization has removed the dependency of the line real loss and reactive storage on voltage. To see this, the AC flow equations for a l, with $\tau_l = 1$, give

$$p_l^{12} + p_l^{21} = g_l(v_{F_l}^2 + v_{T_l}^2) - 2g_l v_{F_l} v_{T_l} \cos\theta_l$$
$$q_l^{12} + q_l^{21} = -(b_l + 0.5b_l^{\text{C}})(v_{F_l}^2 + v_{T_l}^2) + 2b_l v_{F_l} v_{T_l} \cos\theta_l$$

whereas the piecewise linear model gives

$$p_l^{12} + p_l^{21} = 2g_l - 2g_l \cos\theta_l$$
$$q_l^{12} + q_l^{21} = b_l^{\text{C}}(v_{F_l} + v_{T_l} - 1) - 2b_l + 2b_l \cos\theta_l$$

Consequently, the phenomenon of network losses decreasing with higher voltages is not fully captured in the PWL model, and even more degeneracy exists in the PWL OPF problem as to how bus voltages are set. To counter this, higher voltages are encouraged by changing the cost function (1) to

$$\sum_{g\in\mathcal{G}} c_g\left(p_g^{\text{G}}\right) - \epsilon \sum_{b\in\mathcal{B}} v_b - 1, \tag{7}$$

where $\epsilon \geq 0$ should be chosen so as to not make a significant change to the optimal generation cost. For the 24-bus problem, the PWL OPF was re-solved with $\epsilon = 500$. Fig. 3 shows that the errors in voltage and reactive power are reduced. The new generation cost was \$63412—a \$124 increase over the optimal PWL cost, and now an overestimate of AC cost by \$60 (0.10%). The voltage penalty term was 431, *i.e.*, 0.7% of the generation cost.

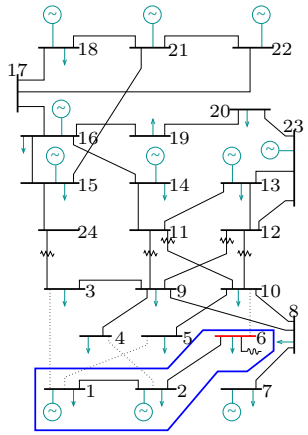

Fig. 4. IEEE 24-bus Reliability Test System, with bus 6 islanded.

III. A Formulation for System Islanding Using Piecewise Linear AC Power Flow

In [12], the problem of determining how to split a transmission network into islands is considered. The aim is to mitigate, for example, the effects of cascading failures and prevent the onset of wide-area blackouts by re-configuring the network—*via* line switching—so that problem areas are isolated. The MILP-based method defines two *sections* of the network: section 0 is to contain all components that are to be isolated, *i.e.*, buses and lines suspected of having faults, and section 1 everything else. The optimization determines which lines to switch, which buses and lines to place in section 0, and where exactly to draw the section boundaries, with the overall objective of minimizing the load that needs to be shed post-islanding to maintain balance. Thus, loads will be fully or partly shed and generators will be adjusted, as appropriate, to establish load-generation balance and respect network equations and operating constraints after the split.

A. Motivation: effect of topology changes on voltage profile

Solution of the MILP islanding problem provides a set of lines to switch, loads to shed and generators to adjust. However, because only the DC power flow equations are included in the constraints, the effects of changing the network topology on voltages and reactive power flows is not considered. Thus, in [12], an AC optimal load shedding (OLS) problem is solved *after* the MILP islanding problem, using the islanded network topology. If a solution to this can be found, the islanded network is feasible with respect to AC power flow and operating constraints. The solution provides the correct generator output and load adjustments to make, now having considered voltage and reactive power.

However, in [12] a number of islanding solutions were found to be AC infeasible. Investigation found the primary cause of infeasibility to be the voltage bounds; a solution can be recovered, albeit with abnormally high or low voltages, by relaxing the normal limits. One such example, for the IEEE RTS, is described as follows. Given the problem of isolating bus 6 while minimizing the expected load shed or lost, the optimal solution islands buses 1, 2 and 6, as indicated in

Fig. 4. There remains sufficient real power capacity in both islands to meet demand, and no load is shed. Moreover, but not by design, there is sufficient reactive power capacity in each island to meet the total reactive power demand. Despite this, a feasible solution to the AC-OLS can not be found. Softening the voltage constraints allows a solution to be recovered, but with an abnormally low voltage of 0.6443 p.u. at bus 6 and an over-limit flow on line $(2, 6)$. Further inspection reveals that this situation has arisen because of the disconnection of line $(6, 10)$, a cable with high shunt capacitance. The passive shunt reactor at bus 6 would, in normal circumstances, balance locally the excess reactive power and maintain a satisfactory voltage profile. A pragmatic approach to islanding would know to either avoid disconnecting $(6, 10)$, or, in the event of its disconnection, switch out the shunt reactor at 6. However, such rules are difficult to collate and encode in automatic islanding or transmission switching algorithms.

This is just one example of where an islanding solution formed by considering only real power—even if network constraints are included—is unsatisfactory. It also shows that even if reactive power balance is achieved within each island, local shortages or surpluses can lead to an abnormal voltage profile. Many test networks are prone to this problem [12]. Moreover, it is not just system islanding that is susceptible; DC-based transmission switching also does not consider the consequences on voltage of disconnecting lines. Thus, there is a need for network topology optimization methods that can determine AC-feasible solutions, but without having to resort to solving the full MINLP problem. The focus of this paper is topology optimization for the purpose of islanding, and in the next section, a formulation is presented that uses the PWL model of AC power flow.

B. Formulation of constraints for islanding

The islanding formulation is developed in this section. The problem is to decide which lines to switch in order to isolate a part of the network. Separation of sections is enforced by sectioning constraints. The islanded network must be balanced, satisfy power flow equations and operating limits in its new state, and so these are included as constraints in the problem.

1) Sectioning constraints: Define $\mathcal{B}^0$ and $\mathcal{B}^1$, where $\mathcal{B}^0 \cap \mathcal{B}^1 = \emptyset$, as the subsets of buses that are desired to be separated. For now, the motivation for this separation is left open, but it may be that these buses in, say, $\mathcal{B}^0$ represent a failing area of the network, or are associated with a coherent group of synchronous machines that will be separated from other groups. The proposed approach will split the network into two *sections*: sections 0 and 1 will contain those buses in $\mathcal{B}^0$ and $\mathcal{B}^1$ respectively. Accordingly, with each bus b is associated a binary variable γ_b, which denotes the section (0 or 1) to which that bus is assigned. That is, if b is to be placed in section 0, then $\gamma_b = 0$. Separation between sections is achieved by switching lines: with each line l is associated a binary variable ρ_l, whose value denotes the connection status of the line. The convention followed is for $\rho_l = 0$ to denote that line l is cut. The exact boundaries of each section will depend on the objective function, defined later, and the optimization will determine how to assign buses not in $\mathcal{B}^0$ or $\mathcal{B}^1$ in order achieve balance and optimize the objective. However, the following constraints enforce the separation of sections 0 and 1.

$$\rho_l \leq 1 + \gamma_{F_l} - \gamma_{T_l}, \forall l \in \mathcal{L}, \tag{8a}$$
$$\rho_l \leq 1 - \gamma_{F_l} + \gamma_{T_l}, \forall l \in \mathcal{L}, \tag{8b}$$
$$\gamma_b = 0, \forall b \in \mathcal{B}^0, \tag{8c}$$
$$\gamma_b = 1, \forall b \in \mathcal{B}^1. \tag{8d}$$

2) Power flow: The remainder of the constraints are concerned with achieving a balanced, steady state for the islanded network. It is assumed that generators are permitted to make only small-scale changes to output or be switched off, and loads may be fully or partly shed in order to maintain a balance. As a consequence of these changes and the topological changes, bus voltages, angles and line flows will change, and so must be modelled to ensure satisfaction of network constraints and operating limits.

First, the power balances, (2a) and (2b), are included without modification. Secondly, the line flow equations are modified so that when a line is disconnected, power flows across it are zero irrespective of the bus voltages and angles at its ends. Introduce auxiliary variables $\hat{p}_l^{ij}$ and $\hat{q}_l^{ij}$, which are equal to the flows that would be induced in a line by its bus voltages and angles:

$$\hat{p}_l^{ij} = G_l^{ii}(2v_l^i - 1) + G_l^{ij}\left(v_l^i + v_l^j + y_l - 2\right) + B_l^{ij}\theta_l, \tag{9a}$$
$$\hat{q}_l^{ij} = B_l^{ii}(1 - 2v_l^i) - B_l^{ij}\left(v_l^i + v_l^j + y_l - 2\right) + G_l^{ij}\theta_l, \tag{9b}$$

for all $l \in \mathcal{L}$ and $i, j \in \{1, 2\} : i \neq j$, where v_l^i and v_l^j are the end voltages of line l, and θ_l is the angle across it. The variable y_l is obtained as the N-piece PWL approximation to $\cos\theta_l$: $\forall l \in \mathcal{L}$,

$$y_l = c_{l,i}\theta_l + d_{l,i}, \forall \theta_l \in [x_i, x_{i+1}], i \in \{0, \ldots, N-1\}. \tag{10}$$

The following constraints control the relationship between bus variables and line-end variables. For all $l \in \mathcal{L}$,

$$-\Theta_l\rho_l \leq \theta_l \leq \Theta_l\rho_l, \tag{11a}$$
$$-\Theta_l^+(1-\rho_l) \leq \theta_l - \delta_{F_l} + \delta_{T_l} \leq \Theta_l^+(1-\rho_l), \tag{11b}$$
$$v_{F_l} - v_l^i \geq (V_{F_l}^{\min} - V_{F_l}^{\max})(1-\rho_l), \tag{11c}$$
$$v_{T_l} - v_l^j \geq (V_{F_l}^{\min} - V_{F_l}^{\max})(1-\rho_l), \tag{11d}$$
$$V_{F_l}^{\min} \leq v_l^i \leq V_{F_l}^{\min} + (V_{F_l}^{\max} - V_{F_l}^{\min})\rho_l, \tag{11e}$$
$$V_{T_l}^{\min} \leq v_l^j \leq V_{T_l}^{\min} + (V_{T_l}^{\max} - V_{T_l}^{\min})\rho_l, \tag{11f}$$
$$V_b^{\min} \leq v_b \leq V_b^{\max}, \forall b \in \mathcal{B}, \tag{11g}$$

where Θ_l is the maximum permissible angle difference across a connected line l, $\Theta_l^+ \geq \Theta_l$ is a "big-M" constant. Of these, (11a) and (11b) force equality of θ_l and $\delta_{F_l} - \delta_{T_l}$ for a connected line, but set $\theta_l = 0$ for a disconnected line while allowing the *bus* angles δ_{F_l} and δ_{T_l} to vary independently. Note that since $\theta_l = 0$ if $\rho_l = 0$, then $y_l = 0$ for a disconnected line. Likewise, if $\rho_l = 1$ then, by (11c) and (11d), $v_l^i = v_{F_l}$ and $v_l^j = v_{T_l}$. However, if $\rho_l = 0$ then $v_l^i = V_{F_l}^{\min}$ and $v_l^j = V_{T_l}^{\min}$.

Finally, the actual flows p_l^{ij} and q_l^{ij} are obtained from $\hat{p}_l^{ij}$ and $\hat{q}_l^{ij}$ by

$$p_l^{ij} = \hat{p}_l^{ij} - P_l^{ij}(1-\rho_l), \tag{12a}$$
$$q_l^{ij} = \hat{q}_l^{ij} - Q_l^{ij}(1-\rho_l), \tag{12b}$$

where $P_l^{ij} = G_l^{ii}(2V_{F_l}^{\min}-1) + G_l^{ij}(V_{F_l}^{\min}+V_{T_l}^{\min}-1)$ and $Q_l^{ij} = B_l^{ii}(1-2V_{F_l}^{\min}) + -B_l^{ij}(V_{F_l}^{\min}+V_{T_l}^{\min}-1)$ are constants and correspond to flows at minimum voltage and zero angle.

3) Operating constraints: In the short time available when islanding in response to a contingency, it is assumed that it is not possible to start up generators. A generator that is operating can either have its input mechanical power disconnected, in which case real output power drops to zero in steady state, or its output can be commanded to a new value within a small interval, $\left[P_g^{\mathrm{G}-}, P_g^{\mathrm{G}+}\right]$, say, for generator g, around the pre-islanded value. The limits will depend on the ramp and output limits of the generator, and the amount of immediate or short-term reserve capacity available to the generator. For reactive power, it is assumed that a new output can be commanded in the range $Q_g^{\mathrm{G}-}$ to $Q_g^{\mathrm{G}+}$, independent of real power output. This alternative operating regime is modelled by the constraints

$$\zeta_g P_g^{\mathrm{G}-} \le p_g^{\mathrm{G}} \le \zeta_g P_g^{\mathrm{G}+}, \forall g \in \mathcal{G}, \tag{13a}$$
$$Q_g^{\mathrm{G}-} \le q_g^{\mathrm{G}} \le Q_g^{\mathrm{G}+}, \forall g \in \mathcal{G}, \tag{13b}$$
$$\zeta_g = 1, \forall g \in \mathcal{G} : P_g^{\mathrm{G}-} = 0, \tag{13c}$$
$$\zeta_g = 1, \forall g \in \mathcal{G}^1. \tag{13d}$$

Here, ζ_g is a binary variable and denotes the on/off setting of the real power output, and $\mathcal{G}^1$ is a subset of generators which are required to remain on.

For loads, because of the limits on generator outputs and network constraints, it may not be possible after islanding to fully supply all loads. It is therefore assumed that some shedding of loads is permissible. Note that this is *intentional* shedding, not automatic shedding as a result of low voltages or frequency. To implement this in the real network there has to be central control over equipment. For all $d \in \mathcal{D}$,

$$p_d^{\mathrm{D}} = \alpha_d P_d^{\mathrm{D}}, \tag{13e}$$
$$q_d^{\mathrm{D}} = \alpha_d Q_d^{\mathrm{D}}. \tag{13f}$$

Finally, line limits are applied in the same way as described for the PWL AC OPF; that is, a limit on ξ_l, corresponding to a limit on heating or current. For all $l \in \mathcal{L}$,

$$p_l^{12} + p_l^{21} \le \frac{g_l}{g_l^2+b_l^2}(S_l^{\max})^2. \tag{13g}$$

C. Objective functions for islanding

The general aim is to split the network, separating the two sections 0 and 1, yet leaving it in a feasible state of operation. The specific motivations and objectives for islanding are discussed in this section. Clearly, if a network can be partitioned with minimal disruption to load, and with minimal disturbances to generators, then its chances of viable operation until future restoration are increased.

1) Isolating uncertain components and maximizing expected load supply: Similar to the approach in [12], the set $\mathcal{B}^0$ may represent those buses that are suspected of having a fault or being at imminent risk of failure (*e.g.*, by cascading failures). There may also be a suspected subset, $\mathcal{L}^0$, of lines. In this situation, it is desired to isolate those buses in $\mathcal{B}^0$ from the rest of the network, and the sectioning constraints ensure this. Any uncertain lines $l \in \mathcal{L}^0$ that remain in section 1, with the "healthy" buses, are disconnected with the additional constraints

$$\rho_l \le 1 - \gamma_{F_l}, \forall l \in \mathcal{L}^0, \tag{14a}$$
$$\rho_l \le 1 - \gamma_{T_l}, \forall l \in \mathcal{L}^0. \tag{14b}$$

Because section 0 is vulnerable, containing the uncertain or failing components, it is assumed that there is a risk of not being able to supply power any load placed in that section. Accordingly, a load loss penalty $0 \le \beta_d < 1$ is defined for a load d, which may be interpreted as the probability of being able to supply a load if placed in section 0. Suppose a reward R_d is obtained per unit supply of load d. If d is placed in section 1 a reward R_d is realized per unit supply; however, if d is placed in section 0, a lower reward of $\beta_d R_d < R_d$ is realized. The objective is then to maximize the expected total value of load supplied:

$$\max \sum_{d\in\mathcal{D}} R_d P_d^{\mathrm{D}}(\beta_d \alpha_{0d} + \alpha_{1d}), \tag{15}$$

where $\alpha_d = \alpha_{0d} + \alpha_{1d}$, and $0 \le \alpha_{1d} \le \gamma_b, \forall b \in \mathcal{B}, d \in \mathcal{D}_b$.

Here a new variable α_{sd} is introduced for the load d delivered in section $s \in \{0,1\}$. If $\gamma_b = 0$ (and so the load at bus b is in section 0), then $\alpha_{1d} = 0$, $\alpha_{0d} = \alpha_d$, and the reward is $\beta_d R_d P_d^{\mathrm{D}} \alpha_d$. Conversely, if $\gamma_b = 1$ then $\alpha_{1d} = \alpha_d$ and $\alpha_{0d} = 0$, giving a larger reward $R_d P_d^{\mathrm{D}} \alpha_d$. Thus, maximizing (15) gives a preference for $\gamma_b = 1$ and a smaller section 0, so that the impacted area is contained.

2) Promoting generator coherency: Another aim is to ensure the synchronicity of generators within islands. Large disturbances in the network cause electro-mechanical oscillations, which can lead to a loss of synchronism. A popular approach is to split the system along boundaries of near-coherent generator groups, as determined by slow-coherency analysis [19]. Thus, weak connections between machines—which give rise to slow, lightly-damped oscillations—are cut, leaving separate networks of tightly-coupled, coherent machines.

Consider those buses in the network with generators attached, the set of which is $\mathcal{B}^{\mathrm{G}} \triangleq \left\{b \in \mathcal{B} : \mathcal{G}_b \neq \emptyset\right\}$, and define $\mathcal{B}^{\mathrm{G,pairs}} \triangleq \left\{\{b,b'\} \in \mathcal{B}^{\mathrm{G}} \times \mathcal{B}^{\mathrm{G}} : b' > b\right\}$ as the set of all pairs of such buses. For what follows, it may be assumed that multiple units at a bus are tightly coupled and are aggregated to a single unit. The dynamic coupling, $W_{bb'}$, between a pair of machines at buses $\{b,b'\} \in \mathcal{B}^{\mathrm{G,pairs}}$ may be determined from slow-coherency analysis. For example [11], assuming the linearized second order swing equation with no damping,

$$W_{bb'} = \frac{\partial(\dot{\omega}_b - \dot{\omega}_{b'})}{\partial \delta_{bb'}} = \left(\frac{1}{M_b} + \frac{1}{M_{b'}}\right)\frac{\partial P_{bb'}}{\partial \delta_{bb'}},$$

where M_b, ω_b, δ_b are the inertia constant, angular frequency and rotor angle of the machine at bus b, and $\frac{\partial P_{bb'}}{\partial \delta_{bb'}}$ is the syn-

chronizing power coefficient or "stiffness" between machines at b and b'. To favour, in the objective, separating loosely-coupled generators, introduce a new variable $0 \leq \eta_{bb'} \leq 1$ for all $\{b, b'\} \in \mathcal{B}^{\mathrm{G}}$. Then the constraints

$$\gamma_b - \gamma_{b'} \leq \eta_{bb'}, \tag{16a}$$

$$-\gamma_b + \gamma_{b'} \leq \eta_{bb'}, \tag{16b}$$

set $\eta_{bb'}$ to 1 if generator buses b and b' are in different sections of the network (and hence electrically isolated), but otherwise may be zero. This indicator variable is included in the objective function

$$\min \sum_{\{b,b'\} \in \mathcal{B}^{\mathrm{G}}} W_{bb'} \eta_{bb'}. \tag{17}$$

This gives a preference for placing machines in sections 0 and 1 such that the inter-section pairs have small $W_{bb'}$, *i.e.*, weak coupling, but intra-section pairs have stronger coupling. The objective will tend to favour keeping all machines in the same section; however, to force the machines into two sections, the following constraints are included.

$$1 \leq \sum_{b \in \mathcal{B}^{\mathrm{G}}} \gamma_b \leq n\big(\mathcal{B}^{\mathrm{G}}\big) - 1. \tag{18}$$

This objective may be used in conjunction with (15), so that section 0 is the "unhealthy" section but the objective prefers to not separate strongly-coupled machines. Alternatively, the following implementation splits the network directly into coherent groups, making different use of the sets $\mathcal{B}^0$ and $\mathcal{B}^1$.

3) Splitting into coherent groups: Suppose that coherent groups of generators have been determined, and that assigned to $\mathcal{B}^0$ and $\mathcal{B}^1$ are those buses in $\mathcal{B}^{\mathrm{G}}$ corresponding to machines in different groups. For example, $\mathcal{B}^0$ may contain the controlling group of machines, and $\mathcal{B}^1$ all others. The sectioning constraints will ensure that the machines are separated, but which other buses are assigned to each section is determined by the optimization. The solution that minimizes the amount of load shed can be found by using the objective

$$\max \sum_{d \in \mathcal{D}} \alpha_d P_d^{\mathrm{D}}. \tag{19}$$

Alternatively, to seek a solution that changes the generator outputs the smallest amount from their initial values P_g^{G0}:

$$\min \sum_{g \in \mathcal{G}} t_g \tag{20}$$

where $t_g \geq 0$, $t_g \geq p_g^{\mathrm{G}} - P_g^{\mathrm{G0}}$, and $t_g \geq -p_g^{\mathrm{G}} + P_g^{\mathrm{G0}}, \forall g \in \mathcal{G}$.

This implementation will split the network into two sections. If separation into r sections is required, the optimization can be re-run with a new choice of $\mathcal{B}^0$ and $\mathcal{B}^1$.

4) Penalties: Often there may be multiple feasible solutions with objective values close to the optimum. Including additional penalty terms in the objective—small enough to not significantly affect the primary objective—improves computation by encouraging binary variables to take integral values in the relaxations, and also guides the solution process towards particular solutions. For example, consider the penalty terms (for a maximization problem)

$$-\sum_{l \in \mathcal{L}} W^{\xi} \xi_l - \sum_{l \in \mathcal{L}} W_l^{\mathrm{L}} (1 - \rho_l) - \sum_{g \in \mathcal{G}} W_g^{\mathrm{G}} (1 - \zeta_l) \tag{21}$$

where W^{ξ}, W_l^{L}, W_g^{G} are weights to be chosen appropriately. The first term penalizes $1 - \cos(\theta_l)$, and hence the total line loss. The second penalizes cuts to lines; for example, setting W_l^{L} equal to the some small multiple of the pre-islanding power flow through the line will penalize most heavily disconnections of high-flow lines. The switching-off of generators is be penalized with the final term. If $W_g^{\mathrm{G}} = \epsilon P_g^{\mathrm{G,max}}$ then units are given uniform weighting. If, say, $W_g^{\mathrm{G}} = \epsilon \big(P_g^{\mathrm{G,max}}\big)^2$, then the disconnection of large units is discouraged.

TABLE II
NUMBERS OF AC-INFEASIBLE SOLUTIONS.

n^{B}	9	14	24	30	39	57	118	300
DC [12]	0	2	7	7	9	6	17	72
PWL AC	0	0	0	0	0	0	0	0

IV. COMPUTATIONAL RESULTS

A. Islanding to minimize expected load loss

A set of scenarios was built based on test systems with between 9 and 300 buses. For a network with n^{B} buses, n^{B} scenarios were generated by assigning in turn each single bus to $\mathcal{B}^0$. No assignments were made to $\mathcal{B}^1$. The lower and upper bounds on real power output for generator g, $P_g^{\mathrm{G,min}}$ and $P_g^{\mathrm{G,max}}$, were defined as $\pm 5\%$ of the the pre-islanding output, P_g^{G0}, obtained by solving an AC OPF on the intact network prior to islanding. To offer robustness to modelling errors in the PWL formulation, the lower bound was then raised by 5% of $(P_g^{\mathrm{G,max}} - P_g^{\mathrm{G,min}})$. Reactive power outputs were allowed to vary over their full range.

In the objective function, a value of 0.75 is used for the load loss penalty β_d. The generator coherency objective was not included. The penalties are $W_g^{\mathrm{G}} = 0.01 P_g^{\mathrm{Gmax}}$, $W^{\xi} = 0.1$ and $W_l^{\mathrm{L}} = 0.0025 \sum_d P_d^{\mathrm{D}}$, so that the line-cut penalty is scaled by the total load in the system. For the PWL approximation for a line l, first the angle difference prior to islanding, θ_l^*, is determined from the base-case AC OPF solution, and then 12 pieces are used over $\pm\big(|\theta_l^*| + 10^{\circ}\big)$.

Feasibility of islanding solutions was checked by solving an AC optimal load shedding problem on the islanded network. The generators in this problem were allowed to use the full $\pm 5\%$ range, $\big[P_g^{\mathrm{G,min}}, P_g^{\mathrm{G,max}}\big]$.

1) AC feasibility: Solving the DC islanding MILP problem for this set of scenarios results in a number of AC infeasibilities, as reported in [12] and shown in Tab. II. However, use of the PWL AC formulation, solving problems to a 1% and 0.1% optimality gaps, leads to AC feasible islands—that satisfy normal voltage bounds—in all cases.

2) AC-feasible islanding of 24-bus network: Returning to the example of Section III-A, the PWL AC islanding approach is applied to the problem of islanding bus 6. The optimal solution (0% MIP gap) is shown in Fig. 5. The topology

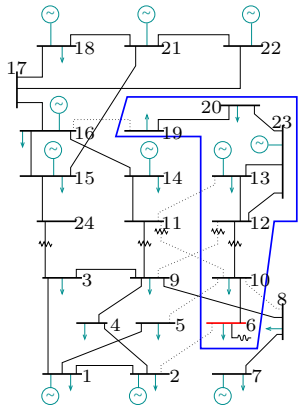

Fig. 5. AC-feasible islanding of the 24-bus network.

TABLE III
COMPARISON OF DC, PWL-AC AND AC-OLS SOLUTIONS.

	DC	PWL-AC	AC-OLS
Exp. load supply (MW)	2764.75	2678.50	2671.15
Generation (MW)	2850.00	2892.33	2884.59
Load supplied (MW)	2850.00	2835.66	2824.87
Line loss (MW)	0.00	56.67	59.72

is significantly different from that in Fig. 4. In particular, the cable $(6, 10)$ is intact. Verification of the solution was performed by solving the AC OLS problem on the islanded network. This problem for the network of Fig. 5 was found to be feasible with normal voltage and line flow bounds. Tab. III compares the solutions obtained by the DC model (from Section III-A), PWL AC model and the post-islanding AC OLS. The PWL AC islanding solution is close to the AC OLS solution. Note that for the DC solution no load was shed; however, the solution was AC infeasible. The PWL AC approach avoids this solution, and achieves AC feasibility at a small cost to load.

3) Computation time: Tab. IV summarizes the computation times for solving the PWL AC islanding problem for the scenarios described in the previous section. Since finding proven optimal solutions is time consuming, problems are solved to a MIP gap of 0.1%, with a 500 s time limit. The table also shows the times to a 1% gap, which are naturally shorter. In practice, since islanding is a measure of last resort, proven optimality is not a priority, and being able to provide good, feasible islands quickly is more important. Times are reported as the total elapsed time (to 1 d.p.) during the solve; the platform was a 64-bit Linux machine with Intel i7-2600 processor and 8 GiB RAM, using CPLEX 12.4 as the solver.

While smaller problems solve very quickly, solve times become non-trivial for larger networks. Since a time limit of 500 s was placed on each optimization, not all 39-, 57-, 118-, and 300-bus problems reached 0.1% optimality. Tab. V shows the optimality gaps at termination for these cases.

B. Coherency-based islanding

The coherency-based splitting approach was applied to the 10-machine, 39-bus New England test network. Slow coherency analysis, assuming second-order dynamics, shows

TABLE IV
TIMES (S) TO SOLVE PWL AC PROBLEMS TO 1% AND 0.1% MIP GAPS.

n^{B}		9	14	24	30	39	57	118	300
1%	Min	0.0	0.0	0.0	0.1	0.0	0.1	0.4	1.2
	Med	0.0	0.3	0.4	0.2	0.5	0.3	0.5	1.5
	Mean	0.0	0.6	0.5	0.9	0.6	28.8	16.5	14.5
	Max	0.0	2.8	1.7	5.8	2.2	500.0	500.0	299.0
0.1%	Min	0.0	0.0	0.1	0.1	0.1	0.1	0.4	1.2
	Med	0.0	0.3	0.5	0.3	0.5	2.1	0.9	1.9
	Mean	0.0	0.7	0.5	1.1	26.3	38.7	28.2	35.2
	Max	0.0	3.0	1.8	6.7	500.0	500.0	500.0	500.0

TABLE V
MIP GAPS (%) OF SOLUTIONS RETURNED AT 500 S.

n^{B}	39	57	118	300
Number	2	4	4	3
Min	0.34	0.21	0.61	0.11
Mean	0.37	2.37	1.22	0.89
Max	0.41	5.12	1.69	2.37

that the machines may be divided into two groups: those at buses 30, 31 and 39 in one group, and then all others.

With $\mathcal{B}^0 = \{31, 34, 39\}$ and $\mathcal{B}^1 = \mathcal{B}^{\mathrm{G}} \setminus \mathcal{B}^0$, the optimal solution splits the system as shown in Tab. VI. The objective was to minimize the movement of generator real power outputs, *i.e.*, (20). To achieve this split and leave the islands balanced, the generator at bus 32 has to lower its output from 671 to 373 MW, while 311 MW is shed. It is worth stating that no other solution exists that splits these two groups of generators but requires less total change in generator outputs.

V. CONCLUSIONS

An optimization-based approach to intentional or controlled islanding has been presented. The approach is flexible with respect to the aims and objectives of islanding, and finds islands that are balanced and satisfy real and reactive power flow and operating constraints. It has been shown that the inclusion of a piecewise linear model of AC power flow allows AC-feasible islands to be found, where previously a DC-based approach led to islands with out-of-bound voltages. Use of objectives that promote generator coherency has been demonstrated.

Future research will focus on heuristics for islanding and improving the computational performance of the approach.

REFERENCES

[1] "Final Report of the Investigation Committee on the 28 September 2003 Blackout in Italy," Union for the Coordination of the Transmission of Electricity (UCTE), Final Report, April 2004.
[2] U.S.-Canada Power System Outage Task Force, "Final Report on the August 14, 2003 Blackout in the United States and Canada: Causes and Recommendations," Final Report, April 2004. [Online]. Available: https://reports.energy.gov/
[3] S. Larsson and A. Danell, "The black-out in southern Sweden and eastern Denmark, September 23, 2003," in *IEEE Power Systems Conference and Exposition*, 2006.
[4] J. W. Bialek, "Lights out?" *IEE Power Engineer*, vol. 19, no. 4, p. 16, August/September 2005.
[5] S. S. Ahmed, N. C. Sarker, A. B. Khairuddin, M. R. B. A. Ghani, and H. Ahmed, "A scheme for controlled islanding to prevent subsequent blackout," *IEEE Transactions on Power Systems*, vol. 18, no. 18, pp. 136–143, February 2003.

TABLE VI
ISLANDING OF 39-BUS NETWORK.

	Section 0	Section 1
Buses	1–9, 30, 31, 39	4, 10–29, 32–38
Generation (MW)	2007.18	3992.29
Load supplied (MW)	1997.89	3945.37
Load shed (MW)	297.21	13.76

[6] K. Sun, D. Z. Zheng, and Q. Lu, "Searching for feasible splitting strategies of controlled system islanding," *IEE Proceedings on Generation, Transmission and Distribution*, vol. 153, pp. 89–98, 2006.

[7] M. Jin, T. S. Sidhu, and K. Sun, "A new system splitting scheme based on the unified stability control framework," *IEEE Transactions on Power Systems*, vol. 22, no. 1, pp. 433–441, February 2007.

[8] B. Yang, V. Vittal, G. T. Heydt, and A. Sen, "A novel slow coherency based graph theoretic islanding strategy," in *IEEE Power Engineering Society General Meeting*, 2007.

[9] L. Liu, W. Liu, D. A. Cartes, and I.-Y. Chung, "Slow coherency and angle modulated particle swarm optimization based islanding of large-scale power systems," *Advanced Engineering Informatics*, vol. 23, no. 1, pp. 45–56, 2009.

[10] C. G. Wang, B. H. Zhang, Z. G. Hao, J. Shu, P. Li, and Z. Q. Bo, "A novel real-time searching method for power system splitting boundary," *IEEE Transactions on Power Systems*, vol. 25, no. 4, pp. 1902–1909, November 2010.

[11] L. Ding, F. M. Gonzalez-Longatt, P. Wall, and V. Terzija, "Two-step spectral clustering controlled islanding algorithm," *IEEE Transactions on Power Systems*, vol. 28, pp. 75–84, February 2013.

[12] P. A. Trodden, W. A. Bukhsh, A. Grothey, and K. I. M. McKinnon, "MILP formulation for controlled islanding of power networks," *International Journal of Electrical Power & Energy Systems*, vol. 45, pp. 501–508, February 2013.

[13] K. W. Hedman, S. S. Oren, and R. P. O'Neill, "A review of transmission switching and network topology optimization," in *IEEE Power and Energy Society General Meeting*, 2011.

[14] B. Stott, J. Jardim, and O. Alsaç, "DC power flow revisited," *IEEE Transactions on Power Systems*, vol. 24, pp. 1290–1300, 2009.

[15] C. Coffrin, P. Van Hentenryck, and R. Bent, "Approximating line losses and apparent power in AC power flow linearizations," in *Proceedings of the 2012 IEEE Power & Energy Society General Meeting*, 2012.

[16] E. M. L. Beale and J. J. H. Forrest, "Global optimization using special ordered sets," *Mathematical Programming*, vol. 10, pp. 52–69, 1976.

[17] R. D. Zimmerman, C. E. Murillo-Sánchez, and D. Gan, *MATPOWER 4.1: A MATLAB power system simulation toolbox*, 2011.

[18] Reliability Test System Task Force of the Application of Probability Methods Subcommittee, "IEEE reliability test system," *IEEE Transactions on Power Apparatus and Systems*, vol. PAS-98, no. 6, pp. 2047–2054, 1979.

[19] B. Avramovic, P. K. Kokotovic, J. R. Winkelman, and J. H. Chow, "Area decomposition for electromechnical models of power systems," *Automatica*, vol. 16, pp. 637–648, 1980.